Restricted Conformational Flexibility of Furanose Derivatives: Ab Initio Interpretation of Their Nuclear Spin−Spin Coupling Constants

Petr Bouř,[*,†,‡] **Ivan Raich,**[‡] **Jakub Kaminský,**[‡] **Richard Hrabal,**[‡] **Jan Čejka,**[‡] **and Vladimír Sychrovský**[†]

Institute of Organic Chemistry and Biochemistry, Academy of Sciences of the Czech Republic, Flemingovo nám. 2, 166 10, Prague 6, Czech Republic, and Department of Analytical Chemistry, Department of Chemistry of Natural Compounds, NMR Laboratory, Department of Solid State Chemistry, Institute of Chemical Technology, Technická 5, 166 28 Prague 6, Czech Republic

Received: December 15, 2003; In Final Form: May 21, 2004

Indirect spin−spin NMR ^1H−^1H coupling constants of newly synthesized furanose monosaccharide derivatives were interpreted on the basis of ab initio modeling. Epoxy, epithio, and epimino groups were inserted into the sugars and significantly limited their conformational flexibility, which was confirmed by a systematic conformer analysis. Because of the restriction, the performance of the computations and the dependence of the coupling constants on the geometry could be estimated more easily. Conventional Karplus equations are not optimized for this class of compounds and cannot be used for reliable interpretation of the NMR spectra. Fully analytical B3LYP/IGLOII computations of the coupling constants were performed including all the four important magnetic terms (SD, DSO, PSO, FC) in the Hamiltonian. Good agreement of the calculated and the experimental coupling constants was achieved, and computed structural parameters are consistent with available X-ray data. The influence of the different functional groups on the spin−spin coupling constants was discussed.

Introduction

A renewed interest in the indirect nuclear spin−spin coupling during the past decade has been partially stimulated by the possibility of modeling experimental constants from the first principles.[1] Indeed, the implementation of the ab initio computational methods for the coupling beyond the conventional Hartree−Fock level brought a decisive improvement of the accuracy, so that the theory could be applied to important chemical problems.[2,3] Especially, the coupled-perturbed approach implemented analytically within the density-functional theory (DFT) led to a substantial decrease of the computational time, so that bigger molecules, solvent effects, and complexes could be studied.[4,5] For some NMR applications the inclusion of the solvent environment into the theory was found important and had to be treated by continuum[6−8] or by explicit solvent models.[9]

Traditionally, empirical relations between the spin−spin coupling constants and molecular geometry, particularly the principal torsion angles in peptides and saccharides, have been used to interpret experimental data.[10−13] This approach, although historically quite successful, bears the danger of failure for systems that deviate from the class of compounds used for calibration of the empirical relations. Also, it may be inappropriate for nonstandard conditions, such as for polar solvents or the formation of molecular aggregates and complexes.

For sugars, the accuracy of NMR spin−spin coupling constants calculated ab initio has been tested only for a relatively small number of methods and with a limited amount of
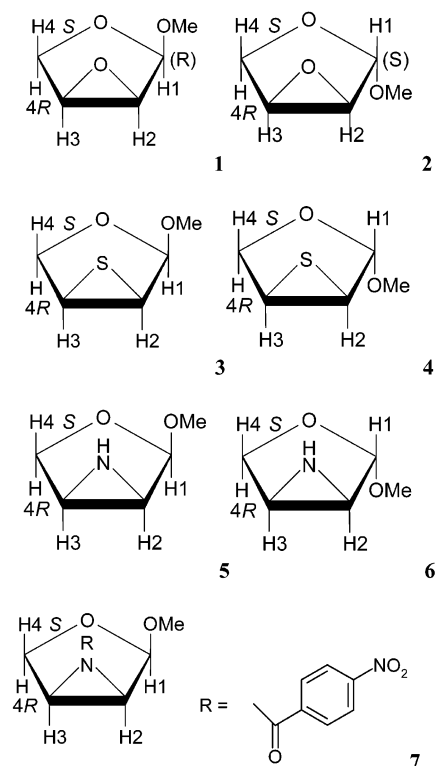
molecules.[14−16] Computed parameters are affected by the level of approximations and quality of the basis sets.[1] For larger saccharides, applications of the more accurate wave function methods (configuration interaction, coupled clusters) is currently not possible. Thus we find it important to assess the performance of the computationally cheaper DFT approach on convenient simple furanose models containing the polar and strained oxirane, thiirane, and aziridine rings. The fusion of these three-membered cycles onto the furanose ring, normally quite flexible in most saccharides, virtually freezes its motion. This possibility makes it convenient for verification of empirical laws relating the NMR parameters to the conformation, for example, although extensive recalibration of the Karplus equations often proposed for flexible systems[16,17] is not reasonable here. As shown below, conformations involving movement of molecular side chains (e.g., CH_3O− group) do not significantly affect the geometry of the furanose ring nor the coupling constants. Several conformers could be excluded on the bases of their calculated relative energies. Most importantly, a particular value of the constant can be assigned to specific torsional angle and, as shown below, the calculations can well discriminate between the individual chemical species.

Presumably, good agreement between computed and experimental coupling constants for the model compounds can further enhance studies of related saccharides. The knowledge of conformational freedom of the furanose ring in sugars is vital for the estimation of biological activity and chemical reactivity.[18] Apart from the broadly used epoxy group,[19] similar functional derivatives with sulfur and nitrogen found important applications in carbohydrate chemistry. For example, episulfides have often been used for the preparation of thio, deoxy, and dideoxy derivatives,[20−23] whereas the epimines are intermediates for the synthesis of various amino and diamino sugars and have been

* To whom correspondence should be addressed. E-mail: bour@uochb.cas.cz. Tel: (420)-220-183-348. Fax: (420)-224-310-503.
† Academy of Sciences.
‡ Institute of Chemical Technology.

Figure 1. Studied compounds: methyl 2,3-anhydro-(α and β)-*l*-erythrofuranoside (**1** and **2**), methyl 2,3-dideoxy-2,3-epithio-(α and β)-*l*-erythrofuranoside (**3** and **4**), methyl 2,3-dideoxy-2,3-epimino-(α and β)-*l*-erythrofuranoside (**5** and **6**), and methyl 2,3-dideoxy-2,3-(4-nitrobenzoylepimino)-α-*l*-erythrofuranoside (**7**). Conventional symbols *S* and *R* are appended to distinguish the hydrogens at positions 4.[30]

established as effective drugs with antiviral and antidiabetic activity.[24−29] The NMR spectroscopy is indispensable for structural studies of these compounds, because many do not crystallize. Particularly, we were able to obtain crystals only of the last of the seven compounds studied here.

Method

We have studied seven furanose epoxy, epithio, and epimino derivatives, particularly methyl 2,3-anhydro-α-*l*-erythrofuranoside (or (1*S*,2*R*,5*S*)-2-methoxy-3,6-dioxabicyclo[3.1.0]hexane by CAS nomenclature, **1**), methyl 2,3-anhydro-β-*l*-erythrofuranoside ((1*S*,2*S*,5*S*)-2-methoxy-3,6-dioxabicyclo[3.1.0]hexane, **2**), methyl 2,3-dideoxy-2,3-epithio-α−*l*-erythrofuranoside ((1*S*,2*R*,5*S*)-2-methoxy-3-oxa-6-thiabicyclo[3.1.0]hexane, **3**) methyl 2,3-dideoxy-2,3-thio-β-*l*-erythrofuranoside ((1*S*,2*S*,5*S*)-2-methoxy-3-oxa-6-thiabicyclo[3.1.0]hexane, **4**) methyl 2,3-dideoxy-2,3-epimino-α-*l*-erythrofuranoside ((1*S*,2*R*,5*S*)-2-methoxy-3-oxa-6-azabicyclo[3.1.0]hexane, **5**), methyl 2,3-dideoxy-2,3-epimino-β-*l*-erythrofuranoside ((1*S*,2*S*,5*S*)-2-methoxy-3-oxa-6-azabicyclo[3.1.0]hexane, **6**), and methyl 2,3-dideoxy-2,3-(4-nitrobenzoylepimino)-α-*l*-erythrofuranoside ((1*S*,2*R*,5*S*)-2-methoxy-6-*N*−(4-nitrobenzoylepimino)-3-oxa-6-azabicyclo[3.1.0]hexane, **7**), structures of which are shown in Figure 1. Using the convention of Serianni and Barker[30] for the C4 protons, hydrogen cis to O3 in **1** is labeled as H4*S* etc.

Details of the synthesis and the X-ray experiment can be found elsewhere and will be elaborated in a separate publication.[31,32] Proton NMR spectra were measured for benzene solutions of the compounds, on the Bruker AM 400 MHz spectrometer, at room temperature. The two- and three-bond proton−proton $^1H-^1H$ indirect NMR coupling constants were obtained by the first-order analysis from the expanded spectra.
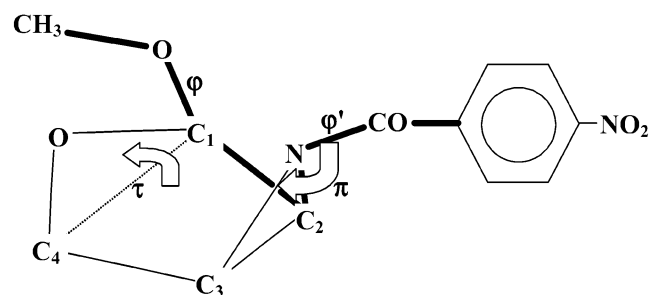
For the derivative number **7** ($C_{12}H_{12}N_2O_5$, the only one that could be crystallized) the monoclinic, space group $P2_1$ (No. 4) was found, with $a = 7.7276(4)$ Å, $b = 15.1967(9)$ Å, $c = 21.1803(7)$ Å, $\beta = 97.490(4)°$, and $V = 2466.1(2)$ Å^3. The structure was solved by direct methods and anisotropically refined by full-matrix least squares. Hydrogen atoms were located from the expected geometry. The Prince modified Chebychev polynomial weighting scheme[33] was used, the refinement converged to $R = 0.0463$ and $R_w = 0.0511$, $S = 1.158$ with the largest residual peaks of -0.35 and $+0.35$ e Å^{-3}. The absolute structure was verified by a Flack enantiopole parameter value of $-0.16(19)$. An extinction parameter of 535-(19) was applied. RC93,[34] SIR92,[35] and CRYSTALS[36] programs were used for data reduction, structure solution, and final refinement.[37]

A systematic conformer search (considering all the free dihedral angles, the furanose ring flipping and the nitrogen pyramidicity for **7**) has been performed. Fully relaxed geometries were optimized with the HF, MP2,[38] and DFT methods using the 4-31G, 6-31G**, and 6-311++G** Pople-style basis sets of Gaussian.[39] The hybrid Becke-3LYP (B3L)[40] and the general gradient approximation (GGA) BPW91[41] DFT functionals were employed for the geometry optimization. The COSMO continuum model[42] was utilized in the optimization to estimate the influence of the benzene solvent on molecular geometries and energies. Supposedly, the model satisfactorily reproduces the electrostatic effect of the solvent on the molecule, because the benzene permittivity is small and does not interact strongly with the solute. The calculation of NMR spin−spin coupling constants was performed with the coupled perturbed DFT method in a vacuum.[2] Note that recent application of polarizible continuum solvent model for the coupling did not bring unambiguous improvement.[43] The coupling constants $^nJ_{a,b}$ (where n is the number of chemical bonds between the protons a and b) were calculated as sums of the four contributions: diamagnetic spin−orbit (DSO), paramagnetic spin−orbit (PSO), Fermi contact (FC), and spin dipolar (SD) terms.[44] Standard 4-31G, 6-31G**, 6-311G**, 6-311++G**, and aug-cc-pVDZ atomic bases, and NMR-optimized basis sets IGLO II and IGLO III developed by Kutzelnigg and co-workers[45] were used for the calculation of the coupling constants, within the B3L functional. The Gaussian program package[39] was used for the geometry optimization and the program COLOGNE 99[46] for the coupling constant calculations. Gaussian output also served as an input to the program ROA[53] so that electron densities perturbed by the coupling terms could be visualized.

Results and Discussion

Geometry. Although the three-membered ring significantly reduces the intramolecular motion, the torsion angle φ, as well as the angles τ (between the plane fitted into the four furanose ring carbon atoms and the plane defined by the C−O−C three atom furanose tip) and π (between the NH (NC) bond and the plane of the three membered ring) as defined in Figure 2 may vary. For the *p*-nitrobenzoate **7** we considered also the rotation around the CN bond (monitoring the angle φ'), whereas the carboxyl and nitro group atoms are kept approximately in the benzene ring plane due to the π-electron conjugation. According to these parameters, we have roughly classified possible conformers in Table 1 (a−f for the epithio and epoxy derivatives **1**−**4**, and a−l for the sugar epimines **5**−**7**) and created corresponding initial geometries.

In Table 2, optimized angles and relative conformer energies for the epoxy diastereoisomers **1**−**2** are summarized as obtained

Conformational Flexibility of Furanose Derivatives

J. Phys. Chem. A, Vol. 108, No. 30, 2004 **6367**

Figure 2. Definition of the dihedral angles φ ($CH_3-O-C_1-C_2$) and φ' ($C_2-N-CO-Ar$), the angle τ between the two planes fitted to the three (C_4OC_1) and four ($C_1C_2C_3C_4$) ring atoms, and the angle π between the NH (N–CO) bond and the C_2NC_3 plane. Analogous definition for the φ and τ angles was used for the epoxy and thio derivatives.

TABLE 1: Classification of Initial Conformer Geometries[a]

conformer	τ[b]	φ (deg)	π (deg)[c]
	Derivatives **1–4**		
a	(+)	180	
b	(+)	60	
c	(+)	−60	
d	(−)	180	
e	(−)	60	
f	(−)	−60	
	Derivatives **5–7**[d]		
a	(+)	180	out(−)
b	(+)	−60	out
c	(+)	60	out
d	(+)	180	in(+)
e	(+)	−60	in
f	(+)	60	in
g	(−)	180	out
h	(−)	−60	out
i	(−)	60	out
j	(−)	180	in
k	(−)	−60	in
l	(−)	60	in

[a] See Figure 2 for the definition of the angles τ, π, and φ. [b] Positive when the oxygen plane (C_1C_4O in Figure 2) points toward the three-member ring ($\tau \sim \pm 20°$) and vice versa. [c] Pyramidal arrangement, out (or negative) when the hydrogen atom points out of the molecular center. [d] Additionally for **7**, the angle φ' (Figure 2) was varied (+60°, −60°, +180°), so that a total of 36 initial conformers were investigated.

at the HF/4-31G, HF/6-311++G**, B3L/6-311++G**, BPW91/6-311++G**, BPW91/6-311++G**/COSMO, and MP2/6-311++G** levels of approximation. Although for **1** three (a–c) (with even four with the MP2/6-311++G** method) stable structures were predicted, only two (a, b) were found for **2**. Additionally, for the latter, an occurrence of the conformation (b) in the sample can be with a high probability excluded, because its relative energy given by all the methods is well separated from the ground-state a. Note that the difference (3.2–4.4 kcal/mol) is bigger than the Boltzmann quantum $kT \sim 0.6$ kcal/mol, as well as the expected accuracy of the calculations (~1 kcal/mol). On the contrary, the computations suggest that conformers a and c are almost equally probable for **1**. Conformer c has even lower relative energy if optimized at the MP2 level. This corresponds to a relatively loose methoxy group that can rotate around a single bond. The motion will be probably even more enhanced by dynamical influence of the solvent, which is, unfortunately, impossible to model by current means. For **1**, the conformation e is favored by the HF/4-31G method, but according to the more advanced methods, it is either not stable or possesses higher energy. Thus we can conclude that the furanose five-atom ring is virtually rigid, which was also one

TABLE 2: Optimized Geometry Parameters and Relative Conformer Energies for the Epoxy Compounds 1 and 2[a]

starting conformer	HF[b]	HF	B3L	BPW	BPW[c]	MP2
			1			
			φ/τ (deg)			
a	173/7	179/20	178/19	176/20	173/21	180/24
b	e	78/18	81/16	85/17	87/21	72/21
c	−69/15	−60/24	−58/23	−57/24	−54/25	−54/28
d	a	a	a	a	a	a
e	62/−13	b	b	b	b	61/−24
f	c	c	c	c	c	c
			E (kcal/mol)			
a	0	0	0	0	0	0
b	-	3.6	3.3	3.0	2.5	3.5
c	5.4	0.3	0.1	0.0	0.5	−0.5
e	−1.3					3.6
			2			
			φ/τ (deg)			
a	178/19	−177/23	−177/24	−176/25	−174/25	−179/28
b	77/10	68/13	66/14	65/16	62/16	66/18
c	a	a	a	a	a	a
d	a	a	a	a	a	a
e	b	b	b	b	b	b
f	a	a	a	a	a	a
			E (kcal/mol)			
a	0	0	0	0	0	0
b	4.0	4.4	3.8	3.6	3.2	3.5

[a] The resultant conformer is indicated when the starting conformer type (Table 1) was not stable. Except of the first HF calculation, the 6-311++G** basis was used. [b] 4-31G basis. [c] COSMO model for the benzene solvent.

of the purposes of the insertion of the epoxy group in the furanose molecule. Compounds **1** and **2** did not form crystals in our hands. However, computed geometry parameters are consistent with X-ray data of two related epoxyfuranose derivatives.[47,48] For the two crystal structures, found values for τ were 19 and 8, and −56 and 48° for φ, respectively. These values of τ are reasonably close to those obtained for the lowest energy conformers a and c, and clearly much smaller than for "normal" furanoses without the epoxy constraint, for which $\tau \sim 35°$, although other coordinates are more apporpriate for description of the flexible ring puckerings.[15] The angle φ is obviously quite vulnerable to the molecular environment, and the experimental data as well as the computations suggest that in principle all the conformations corresponding approximately to the periodic minima (~60, −60, and +180°) are possible for this class of compounds.

Conformer relative energies of the thio derivatives **3** and **4** were calculated only with the two most advanced B3L/6-311++G** and MP2/6-311++G** methods. The optimized geometry parameters and conformer energies are listed in Table 3. Unlike for **1** and **2**, only one conformer seems to be preferred both for **3** and **4** diastereoisomers, although other higher energy conformers (local minima) are possible. Similarly, as for **1** and **2**, the furanose ring in a bicyclic system seems to be quite rigid, with the angles $\varphi \sim 180°$ and $\tau \sim 25$–30°. The sulfur bridge plane is more coplanar with the furanose four carbon plane (the angle between the planes is ~68°) than the epoxy bridge (with the analogous angle of ~73°). To our knowledge, no X-ray data are available for these structures.

Computed conformer energies and geometry parameters for the epimino derivatives **5** and **6** are summarized in Table 4. Despite an additional degree of freedom, the pyramidicity of the nitrogen, and consequently, more local minima, relative

6368 *J. Phys. Chem. A, Vol. 108, No. 30, 2004*

Bouř et al.

TABLE 3: Optimized Geometry Parameters and Conformer Energies for Epithio Derivatives 3 and 4[a]

starting conformer	B3L/6-311++G**	MP2/6-311++G**
	3	
	φ/τ (deg)	
a	176/25	178/31
b	−63/30	−58/35
c	77/24	68/29
d	a	177/−24
e	b	b
f	c	70/−31
	E (kcal/mol)	
a	0	0
b	1.6	1.2
c	3.3	3.3
d		2.3
f		4.8
	4	
	φ/τ (deg)	
a	−177/27	180/32
b	−92/26	−86/31
c	66/17	67/21
d	a	a
e	b	b
f	c	c
	E (kcal/mol)	
a	0	0
b	3.2	3.7
c	4.0	3.9

[a] Similarly as in Table 2, types of the resultant conformations are indicated for unstable starting structures.

TABLE 4: Optimized Geometry Parameters and Conformer Energies for Epimino Derivatives 5 and 6

starting conformer	**5**		**6**	
	B3L	MP2	B3L	MP2
	$\varphi/\tau/\pi$ (deg)			
a	−177/19/−67	180/25/−69	177/24/−68	179/28/−69
b	−78/16/−67	−69/22/−69	−66/14/−67	−66/18/−69
c	60/24/−68	55/29/−70	94/23/−67	87/27/−69
d	176/27/66	−179/31/67	175/31/66	178/34/68
e	−80/24/66	−70/29/68	−63/21/66	−64/24/68
f	55/33/66	53/35/68	97/30/66	85/34/68
g	a	a	a	a
h	b	−62/−29/−69	b	b
i	c	c	c	c
j	d	−179/−21/67	d	d
k	e	−68/−19/68	e	e
l	f	f	f	f
	E (kcal/mol)			
a	3.6	4.1	1.8	2.3
b	7.0	7.6	5.4	5.5
c	3.9	3.8	5.4	6.4
d	0.0	0.0	0.0	0.0
e	3.0	3.0	4.1	3.8
f	2.3	1.5	3.6	4.0
h		7.3		
j		1.9		
k		4.3		

conformer energies suggest that one conformation is prevalent, similarly as for **1**−**4**. For the lowest energy conformer (d) the furanose ring oxygen tip (see angle τ) points to the three-member ring, similarly as for the most stable forms of **1**−**4**. For **5**, flipping of the oxygen tip of the ring is enhanced by forming an intramolecular hydrogen bond with the NH group, which results in a relatively low energy 1.9 kcal/mol obtained for the conformer j, whereas for **1**−**4** such conformations are either not stable at all or are associated with an energy increase of

TABLE 5: Relative Energies and Geometric Parameters for Five Lowest Energy Conformers of Derivative 7

level	*E* (kcal/mol)	φ (deg)	τ (deg)	π (deg)	φ' (deg)
		I			
HF/4-31G	0	−174	10	44	70
B3L/6-31G**	0	179	21	52	77
B3L/6-311++G**	0	177	20	51	75
		II			
HF/4-31G	0.7	−176	17	−35	−67
B3L/6-31G**	0.9	177	30	−44	−70
B3L/6-311++G**	1.2	175	29	−43	−68
		III			
HF/4-31G	4.4	−176	11	46	−163
B3L/6-31G**	2.6	176	23	54	−155
B3L/6-311++G**	2.1	176	22	53	−154
		IV			
HF/4-31G	4.5	−64	22	44	−155
B3L/6-31G**	2.7	−55	28	52	−150
B3L/6-311++G**	2.9	−56	28	51	−150
		V			
HF/4-31G	7.0	−175	26	−26	151
B3L/6-31G**	4.7	175	30	−44	142
B3L/6-311++G**	5.2	174	33	−39	142
X-ray[a]		172	26	52	76
		177	23	50	69
		177	24	51	68
		174	24	53	76

[a] Four molecules in the elementary cell.

3.5−4.8 kcal/mol. Attempts to crystallize the epimino compounds **5** and **6** were not successful. But angles $\tau = (31°, 8°)$ and $\pi = (51°, 59°)$ found by X-ray for related epiminofuranose derivatives[49,50] correspond consistently to the b conformer (in Table 4). It is also reasonable to suppose that compounds **5** and **6** prefer the conformation d as they can form the intramolecular hydrogen bond between the NH and −O− groups. Additionally, repulsion between the nitrogen and oxygen electron lone pairs may stabilize this conformation.

The last compound **7** is the most flexible, due to the additional *p*-nitrobenzoyl group. Systematic searches preformed at the HF/4-31G and B3LYP/6-31G** levels provided a total of 7 and 10 local minima on the potential energy surface, respectively. Geometry parameters and relative energies of the five lowest energy conformers (I−V, same for both methods) are listed in Table 5. Additionally, these conformers were optimized with a bigger basis (6-311++G**) for the B3L method. The most-favored conformer (I) corresponds to the type d in Table 4 for **6** and **7**, and its theoretical parameters (φ, τ, π, φ') estimated by the DFT method nicely reproduce the X-ray data. Because the relative energy ordering of the first three conformers was same for both methods and confirmed by the computation with the bigger basis, we suppose that conformer I is also prevalent in the liquid state. Obviously, this assumption may not be relevant for polar solvents or for elevated temperatures.

Spin−Spin Coupling Constants. Experimental and calculated coupling constants for **1** and **2** are listed in Table 6. The constants were calculated at the B3L/IGLOII level for the B3L/6-311++G** and MP2/6-311++G** optimized geometries, and at the B3L/IGLOIII level for MP2/6-311++G** optimized geometry. We investigated these combinations because previous computations of the spin−spin couplings utilizing the optimized IGLO II and IGLO III bases did not regard the geometry changes separately.[2,51] As seen in the table, the geometry and basis-set variations cause changes in the constants typically smaller than ∼0.3 Hz. Given the limited precision of computation and experiment, the accuracy is sufficient for practical

Conformational Flexibility of Furanose Derivatives

J. Phys. Chem. A, Vol. 108, No. 30, 2004 **6369**

TABLE 6: Experimental and Calculated[a] Spin−Spin Coupling Constants (Hz) for Epoxy Compounds 1 and 2

	exp (in C_6D_6)	B3L geometries/IGLO II			MP2 geometries/IGLO II				MP2 geometries/IGLO III			
		a	b	c	a	b	c	e	a	b	c	e
					1							
$^3J_{1,2}$	0.7	1.1	0.9	0.9	0.9	0.7	0.7	1.7	0.7	0.5	0.5	1.4
$^3J_{2,3}$	3.0	3.0	2.4	2.5	2.4	2.5	2.5	2.8	2.5	2.7	2.7	3.0
$^3J_{3,4R}$	1.0	1.3	1.4	1.2	1.0	1.2	0.9	3.0	0.9	1.0	0.8	2.8
$^3J_{3,4S}$	<0.5	−0.1	−0.1	0.0	0.0	−0.1	0.0	0.7	0.0	−0.1	0.0	0.8
$^2J_{4R,4S}$	−10.6	−10.5	−10.5	−10.6	−10.0	−10.0	−10.1	−9.9	−8.5	−8.6	−8.7	−8.5
					2							
$^3J_{1,2}$	<0.5	−0.1	−0.1		0.0	−0.1			0.0	0.0		
$^3J_{2,3}$	2.8	2.3	2.2		2.4	2.2			2.6	2.3		
$^3J_{3,4R}$	0.8	1.1	1.3		0.9	1.2			0.8	1.0		
$^3J_{3,4S}$	<0.5	0.0	−0.1		0.0	0.0			−0.1	−0.1		
$^2J_{4R,4S}$	−10.3	−10.1	−10.1		−9.5	−9.6			−8.0	−8.1		
$^4J_{2,4S}$	0.4	0.0	0.1		−0.1	0.1			0.3	0.5		
$^4J_{2,4R}$	0.4	0.1	0.0		0.1	0.1			0.3	0.3		
$^4J_{1,4S}$	−0.7	−0.9	−0.5		−0.9	−0.6			−0.8	−0.5		

[a] By the analytical coupled-perturbed DFT B3L method. Numbering of the hydrogen atoms is given in Figure 1.

TABLE 7: Dependence of Calculated Coupling Constants on the Basis Set for 1[a]

	4-31G 88 b.f.	6-31G** 130 b.f.	6-311G** 192 b.f.	6-311++G** 232 b.f.	IGLO II 232 b.f.	AUG-cc-pvdz 272 b.f.	IGLO III 376 b.f.
$^3J_{1,2}$	1.29	0.55	0.60	0.64	0.67	0.72	0.48
$^3J_{2,3}$	3.04	2.53	2.35	2.52	2.53	1.78	2.70
$^3J_{3,4R}$	1.78	1.04	1.07	1.08	1.16	1.12	1.00
$^3J_{3,4S}$	−0.14	−0.27	−0.19	−0.18	−0.05	−0.21	−0.08
$^2J_{4R,4S}$	−15.25	−10.59	−9.01	−8.94	−10.02	−8.24	−8.60

[a] The MP2/6-311++G** optimized geometry of conformation **1**b was used.

reasons. For benchmark studies, however, such dependence on geometry (using the same IGLO II basis for the coupling calculation) is rather surprising and has to be taken into account. For example, the $J_{2,3}$ constants for the first (a of **1**) conformer were calculated as 3.0 and 2.4 Hz with the B3L and MP2 geometries, respectively, i.e., with a relative error of 20%. Similar errors originate in the basis set dependence, as can be seen by comparison of the IGLO II and IGLO III results. For example, the absolute value of the $J_{4R,4S}$ constant of **1** (conformer a) decreases by 2.1 Hz if calculated in the bigger basis set.

Apparently, it is the relative accuracy that is characteristic for the computed values. This is rather convenient for applications, as the longer range (and on average smaller) coupling constants are more important for elucidation of molecular structure. By comparing of the calculated and experimental vicinal (over three bonds) constants listed in Table 6, we can see that the difference is typically smaller than 15%. Unfortunately, very small constants cannot be reliably determined experimentally.

As follows from general experimental experience, the spin−spin coupling senses molecular geometry locally and the influence of remote groups weakly interacting with the coupled atoms quickly fades. Indeed, as can be observed in Table 6, rotation of the methoxy residue (generating conformers a ↔ b ↔ c) does not change significantly magnitudes of the coupling constants for hydrogens attached to the furanose ring. On the other side, for the conformer e of **1,** where the geometry of the furanose cycle is different than for a−c, significantly different constants are predicted. Because these do not agree with the experiment (e.g., the calculated values $J_{1,2} = 1.4–1.7$, $J_{3,4R} = 2.8–3.0$ Hz are much bigger than the experimental couplings of 0.7 and 1.0 Hz, respectively), we can exclude a presence of this conformer in the sample not only on the basis of the relative energy ordering (Table 2) but also because of the unrealistic theoretical coupling values.

The fidelity of the computations is rather satisfying for practical purposes, e.g., important coupling terms as the $J_{3,4R}$ and $J_{3,4S}$ couplings can be clearly distinguished, which suggests that direct computations can be used for saccharide conformational studies in place of the Karplus equations for interpretation of the experiment. Nevertheless the basis set dependence of the results is still disturbing, because bigger bases make the computations uneconomic and inaccessible for bigger molecules. Convergence of the coupling constants with the basis set size was investigated more systematically, and the results are shown in Table 7 for the MP2/6-311++G** geometry of the **1**b species only. Clearly, except for the simplest 4-31G basis, the accuracy is stabilized within the range mentioned above, but it does not readily improve agreement with the experiment further when the size of the basis set increases. This corresponds to the findings of Helgaker and colleagues[52] and reflects the complexity of the spin−spin coupling phenomenon. Particularly, it is quite difficult to find an economic and balanced basis for all four (diamagnetic, paramagnetic, Fermi, and spin dipolar) relevant Hamiltonian terms. Obviously, in the future, one can expect that reliability of the predictions will be further improved also by taking into account the solvent environment and vibrational and overall dynamical averaging, or by a development of better functional and wave function methods.

The spin−spin coupling constants for the thio and epimino derivatives **3**−**7** were calculated for the B3L/6-311++G** optimized geometry of the lowest energy conformers and at the B3L/IGLOII level for coupled-perturbed calculation and are compared to the experimental values in Table 8. Similarly as for the epoxides **1** and **2**, the theoretical values correctly follow the experimental ordering and magnitudes of the constants, and mostly distinguish between different individual compounds. For example, the $J_{1,2}$ constant is immeasurably small for **4**, **6**, and **7**, but it increases above 1 Hz for **3** and **5**, both in experiment and in the theory. The only inconsistency between the computed and experimental constant $J_{1,2}$ of **7** can be most probably

6370 *J. Phys. Chem. A, Vol. 108, No. 30, 2004*

Bouř et al.

TABLE 8: Experimental and Calculated Spin−Spin Coupling Constants for the Epithio (3 and 4) and Epimino (5−7) Derivatives[a]

	3		**4**	
	exp	B3L/IGLOII	exp	B3L/IGLOII
$^3J_{1,2}$	2.1	2.7	<0.5	−0.1
$^3J_{2,3}$	5.0	4.6	4.8	4.5
$^3J_{3,4R}$	2.6	3.0	1.8	2.8
$^3J_{3,4S}$	<0.5	0.1	<0.5	0.1
$^2J_{4R,4S}$	−10.1	−10.3	−10.2	−10.0

	5		**6**	
	exp	B3L/IGLOII	exp	B3L/IGLOII
$^3J_{1,2}$	1.4	1.7	<0.5	0.0
$^3J_{2,3}$	4.0	3.0	3.9	3.0
$^3J_{3,4R}$	1.7	1.8	1.5	1.7
$^3J_{3,4S}$	<0.5	0.0	<0.5	0.0
$^2J_{4R,4S}$	−9.8	−9.8	−9.2	−9.3

	7	
	exp	B3L/IGLOII
$^3J_{1,2}$	<0.5	1.9
$^3J_{2,3}$	4.4	4.2
$^3J_{3,4R}$	1.4	2.4
$^3J_{3,4S}$	<0.5	0.1
$^2J_{4R,4S}$	−10.1	−9.9

[a] Calculated values are given for the lowest energy conformers.

attributed to an experimental artifact, because the calculated value of 1.9 Hz is consistent with those for the related compounds **1**, **3**, and **5**.

Generally, the vicinal coupling constants are considered to be closely related to the H−C−C−H dihedral angle.[10−13] This is approximately true also for our class of compounds as follows from the overview of the experimental vicinal constants and computed torsional angles in Table 9. Here, the computed angles are also compared to those obtained by Altona's formulation of the Karplus equations.[55] Clearly, there is loose dependence between the coupling constants and the calculated angles, but quantitative conclusions cannot be made. For example, for **1** and **3** the $J_{1,2}$ constants differ by 1.4 Hz (200%) whereas corresponding angles do by 5° (i.e., 10%). Similarly, the constant $J_{3,4R}$ is smallest for **2** and biggest for **3**, whereas compounds **4** and **6** exhibit extreme values of angles.

The values of the torsion angles predicted on the basis of the Karplus equation in Table 9 mostly agree with the presumably correct numbers obtained by the computation for the 1−2 and 3−4R coupling, whereas the angles obtained on the basis of the 2−3 and 3−4S coupling are off by up to 55°. The especially large differences for the 2−3 coupling can be obviously attributed to the influence of the three-member ring, for which the original semiempirical formula could not be adjusted. Also, it is remarkable that the 1−2 torsion angles are much better reproduced by the Karplus formula for all the β-furanosides (**2**, **4**, **6**) than for the α-isomers (**1**, **3**, **5**, **7**). It may indicate nonlocal contribution to the coupling from the methoxy group.

To obtain an intuitive image about such influence of various molecular parts on the indirect spin−spin interaction, we visualized locations of some important coupling terms in Figure 3 for the $J_{2,3}$ constant: the diamagnetic coupling density, and perturbations of the electron density caused by the paramagnetic and Fermi terms from the H2 atom within the sum-over-state (SOS) approximation described previously.[53] Although the SOS method provided systematically underestimated values of the constants,[53] we find it convenient for description of the qualitative trends, because it is simpler and computationally

cheaper than the coupled-perturbed calculation. For the comparison, similar conformers were selected, so that solely the influence of the epoxy, epithio, and epimino groups could be monitored.

The diamagnetic coupling density (top of Figure 3) is apparently mostly localized along the H−C−C−H vicinal system, which corresponds to the usual chemical image of the spin−spin coupling as a local phenomenon. Nevertheless, other atoms contribute to the coupling, too. Particularly, the recognizable contribution of the most distant carbon of the methyl group is rather surprising, as the dipole-operator quickly fades with the distance. However, relative contributions of the remote atoms to the coupling constant are rather minor, as they are roughly proportional to the volumes closed by the isodensity surfaces. Note that the methyl and other groups can contribute to the coupling also indirectly, via electron conjugation, electrostatic field, etc.

The sulfur atom participates more on the DSO coupling than the −O− and −NH− groups. This is in agreement with the DSO part of the $J_{2,3}$ constants, as they are approximately the same for the epoxide and epimine (−0.53 and −0.59 Hz, respectively) whereas its magnitude (in absolute value) decreases to −0.20 Hz for the epithio sugar.

For the density perturbations caused by the paramagnetic term of the hydrogen H2 (middle in Figure 3) relative differences among the three compounds cannot be judged. Nevertheless, we can see that the perturbation is spread over most of the molecule, similarly as is the DSO density. This corresponds to the same underlying spin−orbital interaction providing these two terms. Lately, it has been shown that (at least for light atoms) all orbitals participate on the PSO coupling mechanism.[54] As can be seen from the calculated values, the PSO terms is again smallest for the sulfur-containing compound (0.13 Hz), but similar (0.40 and 0.45 Hz) for the oxirane and aziridine derivatives.

The density perturbation caused by the Fermi contact interaction is displayed at the bottom of Figure 3, for a different projection of the molecule. This term seems to be the most localized and least influenced by the chemical environment. Indeed, the epoxy and epimino derivatives again exhibit similar values of the FC contributions (3.06 and 3.07 Hz) and the term for the epithio sugar (4.54 Hz) differs significantly; nevertheless, the relative change is much smaller than that for the DSO and PSO terms. The minor role of the sulfur atom can be expected in a direct mediation of this interaction, as the perturbed density by the FC term around this atom is noticeably smaller than for the oxygen and nitrogen derivatives. This can be most probably explained by the longer C−S bond lengths of ∼1.83 Å, if compared to the C−N (∼1.47 Å) or C−O (∼1.43 Å) bond lengths. For the FC perturbation, we may also see lobes pointing inside the envelope formed by the furanose and the three-membered rings and not following any σ-bonds, which is rather a counterintuitive phenomenon and can partially explained the difficulties in the basis-set size convergence of the constants (Table 7). Calculated values of the spin-dipolar (SD) contributions are similar and rather negligible for all the compounds, in accord with previous observations for this kind of interaction.[1,2,53]
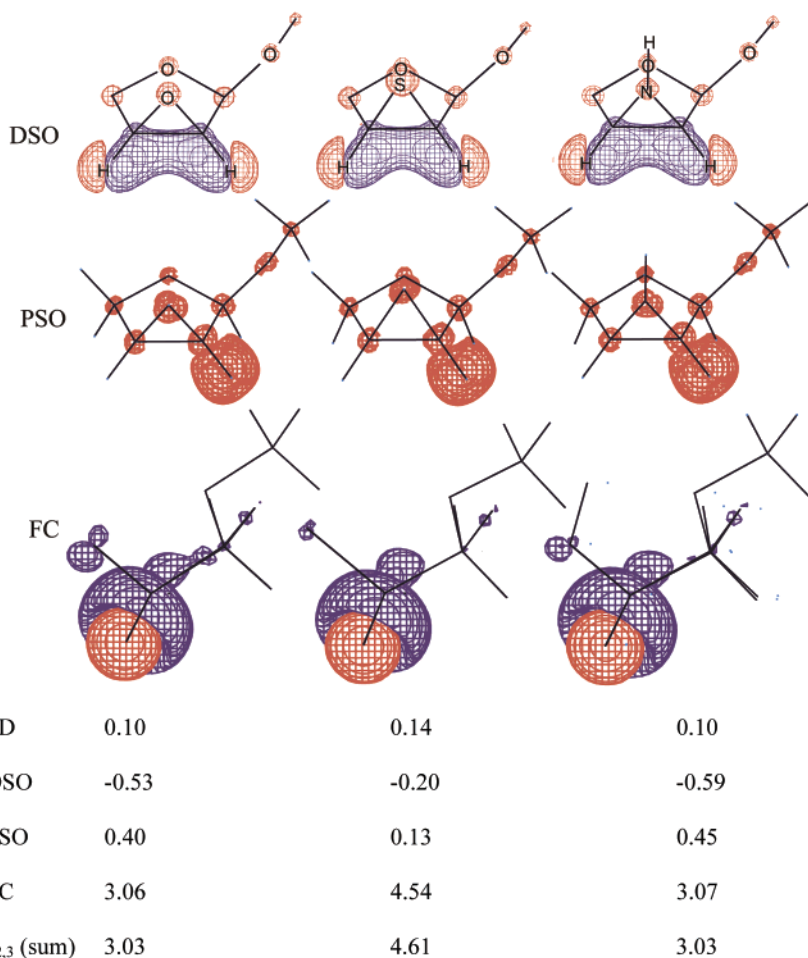
Conclusions

By the insertion of the epoxy −O−, epithio −S−, and epimino −N− groups, the motion of the furanose ring in the model compounds was restricted, which was confirmed by ab initio computations of conformer energies. The restriction

Conformational Flexibility of Furanose Derivatives

J. Phys. Chem. A, Vol. 108, No. 30, 2004 **6371**

TABLE 9: Vicinal H−C−C−H Coupling for All Compounds 1−7 (Experimental Constants and the Dihedral Angles)

H, H	*J* (Hz)							∠ calculated/predicted by Karplus relation[55]						
	1	2	3	4	5	6	7	1	2	3	4	5	6	7
1, 2	0.7	0[b]	2.1	0[b]	1.4	0[b]	0[b]	48	−78	43	−87	46	−77	41
								78[c]	−78[c]	62	−86[c]	68	−83[c]	84[c]
2, 3	3.0	2.8	5.0	4.8	4.0	3.9	4.4	0	1	0	0	1	0	1
								55	56	48	49	51	51	49
3, 4R	1.0	0.8	2.6	1.8	1.7	1.5	1.4	−45	−44	−41	−35	−45	−46	−40
								−99	−102[c]	−71	−79	−85	−88	−90
3, 4S	0[b]	0[b]	0[b]	0[b]	0[b]	0[b]	0[b]	78	79	82	88	77	78	83
								86[c]	86[c]	80[c]	80[c]	81[c]	81[c]	81[c]

[a] The calculated dihedral angles ∠ (HCCH, deg) are given for the lowest energy conformer obtained by the MP2/6-311++G** method. [b] Experimental constant is smaller than ∼0.5 Hz. [c] Experimental couplings were outside the calibrated range (too small).

SD	0.10	0.14	0.10
DSO	-0.53	-0.20	-0.59
PSO	0.40	0.13	0.45
FC	3.06	4.54	3.07
J$_{2,3}$ (sum)	3.03	4.61	3.03

Figure 3. Vicinal $J_{2,3}$ coupling: the diamagnetic spin−orbit (DSO) coupling density ($\rho = 0.001$) and the density perturbations isosurfaces caused by the paramagnetic (PSO, $\partial\rho/\partial\mu = 0.007$) and Fermi contact (FC, $\partial\rho/\partial\mu = 0.002$, different projection) terms of the ^{2}H atom. The signs are indicated by the red (+) and blue (−) colors. Analogous conformers were chosen, from left to right: a of **1**, a of **3**, and d of **5**. Individual contributions of the four Hamiltonian terms to the resulting constants (in Hz) are given at the bottom.

enabled us to better relate the experimental and calculated ^{1}H−^{1}H spin−spin coupling constants to molecular structure, and estimate the influence of the molecular functional groups on the coupling separately. Conventional Karplus equations are not parametrized for this class of compounds exhibiting large deviation from the sp^3 ideal tetrahedral geometry of the carbon orbitals. Indeed, they provided rather unrealistic values of dihedral angles, namely for those derived from the 2−3 coupling involving the bridged atoms. Good agreement was achieved between the experiment and the ab initio results, although residual inaccuracy of the calculated constants (∼15%) could not be overcome by increasing the basis set size. It can be also in part attributed to the error of the ab initio (DFT) method and neglecting of the vibrational effects. The motion of the side

methoxy and NH groups does not have significant influence on the couplings within the furanose ring, and their quantitative analysis is behind capabilities of the modeling because of the limited precision. The dependence of the computed coupling constants on the method used for obtaining the equilibrium geometry was found comparable with the basis set dependence of the coupled-perturbed calculation (with fixed geometry). The visualization of the coupling densities provided a better intuitive picture about the influence of various molecular parts on the vicinal coupling. Predicted geometries are consistent with the available X-ray data.

References and Notes

(1) Helgaker, T.; Jaszunski, M., Ruud, K. *Chem. Rev.* **1999**, *99* (1), 293.

(2) Sychrovský, V.; Gräfenstein, J.; Cremer, D. *J. Chem. Phys.* **2000**, *113*, 3530.

(3) Helgaker, T.; Watson, M.; Handy, N. C. *J. Chem. Phys.* **2000**, *113*, 9402.

(4) Jaszunski, M.; Ruud, K.; Helgaker, T. *Mol. Phys.* **2003**, *101* (13), 1997.

(5) Barone, V.; Peralta, J. E.; Contreras, R. H.; Snyder, J. P. *J. Phys. Chem. A* **2002**, *106*, 5607.

(6) Autschbach, J.; Le Guennic, B. *J. Am. Chem. Soc.* **2003**, *125* (44), 13585.

(7) Sychrovský, V.; Schneider, B.; Hobza, P.; Zídek, L.; Sklenář, V. *Phys. Chem. Chem. Phys.* **2003**, *4*, 734.

(8) Åstrand, P.-O.; Mikkelsen, K. V.; Jørgensen, P.; Ruud, K.; Helgaker, T. *J. Chem. Phys.* **1998**, *108*, 2528.

(9) Autschbach, J.; Ziegler, T. *J. Am. Chem. Soc.* **2001**, *123*, 3341.

(10) Bush, C. A.; Pastor, M. M.; Imberty, A. *Annu. Rev. Biophys. Biomol. Struct.* **1999**, *28*, 269.

(11) Drake, E. N.; Brown, C. E. *J. Chem. Educ.* **1977**, *54*, 124.

(12) Karplus, M. *J. Am. Chem. Soc.* **1963**, *85*, 2870.

(13) Mulloy, B.; Frenkiel, T. A.; Davies, D. B. *Carbohydr. Res.* **1988**, *184*, 39.

(14) Jaworski, A.; Ekiel, I. *Int. J. Quant. Chem.* **1979**, *16*, 615.

(15) Wu, A.; Cremer, D. *Int. J. Mol. Sci.* **2003**, *4*, 158.

(16) Ratajczyk, T.; Pecul, M.; Sadlej, J.; Helgaker, T. *J. Phys. Chem. A* **2004**, *108*, 2758.

(17) Wu, A.; Cremer, D.; Auer, A. A.; Gauss, J. *J. Phys. Chem. A* **2002**, *106*, 657.

(18) Cremer, D.; Pople, J. A. *J. Am. Chem. Soc.* **1975**, *97*, 1354.

(19) Hümmer, W.; Gracza, T.; Jäger, V. *Tetrahedron Lett.* **1989**, *30*, 1517.

(20) Driguez, H.; McAuliffe, J. C.; Stick, R. V.; Tilbrook, D. M. G.; Williams, S. J. *Aust. J. Chem.* **1996**, *49*, 343.

(21) Stick, R. V.; Tilbrook, D. M. G.; Williams, S. J. *Tetrahedron Lett.* **1997**, *38*, 2741.

(22) Stick, R. V.; Tilbrook, D. M. G.; Williams, S. J. *Aust. J. Chem.* **1997**, *50*, 240.

(23) Flores, F. G. C.; Mendoza, P. G.; Mateo, F. H.; Garcia, J. I.; Gonzalez, F. S. *J. Org. Chem.* **1997**, *62*, 3944.

(24) Asano, N.; Nash, R. J.; Molyneux, R. J.; Fleet, G. W. J. *Tetrahedron: Asymmetry* **2000**, *11* (8), 1645.

(25) Winchester, B.; Fleet, G. W. J. *J. Carbohydr. Chem.* **2000**, *19* (4−5), 471.

(26) Winchester, B.; Fleet, G. W. J. *Glycobiology* **1992**, *2* (3), 199.

(27) Butters, T. D.; Dwek, R. A.; Platt, F. M. *Chem. Rev.* **2000**, *100* (12), 4683.

(28) Gruters, R. A.; Neefjes, J. J.; Tersmette, M.; de Goede, R. E. Y.; Tulp, A.; Huisman, H. G.; Miedema, F.; Ploegh, H. L. *Nature* **1987**, *330*, 74.

(29) Fleet, G. W. J.; Karpas, A.; Dwek, R. A.; Fellows, L. E.; Tyms, A. S.; Petursson, S.; Namgoong, S. K.; Ramsden, N. G.; Smith, P. W.; Son, J. C.; Wilson, F.; Witty, D. R.; Jacob, G. S.; Rademacher, T. W. *FEBS Lett.* **1988**, *237*, 128.

(30) Serianni, A. S.; Barker, R. *J. Org. Chem.* **1984**, *49*, 3292.

(31) Raich, I. PhD. Thesis, Institute of Chemical Technology, Prague, 1994.

(32) Jarý, J.; Raich, I. *Carbohydr. Res.* **1993**, *242*, 291.

(33) Prince, E. *Mathematical Techniques in Crystallography and Materials Science*; Springer-Verlag: New York, 1982.

(34) Watkin, D. J.; Prout, C. K.; Lilley, P. M. deQ. *RC93*, Chemical Crystallography Laboratory: Oxford, U.K., 1994.

(35) Altomare, A.; Cascarano, G.; Giacovazzo G.; Guagliardi A.; Burla M. C.; Polidori, G.; Camalli, M. *J. Appl. Crystallogr.* **1994**, *27*, 435.

(36) Betteridge, P. W.; Carruthers, J. R.; Cooper, R. I.; Prout, K.; Watkin, D. J. *J. Appl. Crystallogr.* **2003**, *36*, 1487.

(37) CCDC 235461 contains the supplementary crystallographic data (available via httm://www.ccdc.cam.ac.uk/data_request/cif, by emailing data_request@ccdc.cam.ac.uk, or by contacting The Cambridge Crystallographic Data Centre, 12, Union Road, Cambridge CB2 1EZ, UK; fax: +44 1223 336033.

(38) Møller, C.; Plesset, M. S. *Phys. Rev.* **1934**, *46*, 618.

(39) Frisch, M. J.; Trucks, G. W.; Schlegel, H. B.; Scuseria, G. E.; Robb, M. A.; Cheeseman, J. R.; Zakrzewski, V. G.; Montgomery, J. A.; Stratmann, R. E.; Burant, J. C.; Dapprich, S.; Millam, J. M.; Daniels, A. D.; Kudin, K. N.; Strain, M. C.; Farkas, O.; Tomasi, J.; Barone, V.; Cossi, M.; Cammi, R.; Mennucci, B.; Pomelli, C.; Adamo, C.; Clifford, S.; Ochterski, J.; Petersson, G. A.; Ayala, P. Y.; Cui, Q.; Morokuma, K.; Malick, D. K.; Rabuck, A. D.; Raghavachari, K.; Foresman, J. B.; Cioslowski, J.; Ortiz, J. V.; Stefanov, B. B.; Liu, G.; Liashenko, A; Piskorz, P.; Komaroni, I.; Gomperts, R.; Martin, R. L.; Fox, D. J.; Keith, T.; Al-Laham, M. A.; Peng, C. Y.; Nanayakkara, A.; Gonzales, C.; Challacombe, M.; Gill, P. M. W.; Johnson, B. G.; Chen, W.; Wong, M. W.; Andres, J. L.; Head-Gordon, M.; Replogle, E. S.; Pople, J. A. *Gaussian 98*, revision A.7; Gaussian, Inc.: Pittsburgh PA, 1998.

(40) Becke, A. D. *J. Chem. Phys.* **1993**, *98*, 5648.

(41) Perdew, J. P.; Burke, K.; Wang, Y. *Phys. Rev. B* **1996**, *54*, 16533.

(42) Barone, V.; Cossi, M.; Tomasi, J. *J. Comput. Chem.* **1998**, *19*, 404.

(43) Ruud, K.; Frediani, L.; Cammi, R.; Mennucci, B. *Int. J. Mol. Sci.* **2003**, *4*, 119−134.

(44) Ramsey, N. F. *Phys. Rev.* **1953**, *91*, 303.

(45) Kutzelnigg, W.; Fleischer, U.; Schindler M. *NMR−Basic Principles and Progress*; Springer: Heidelberg, 1990.

(46) Kraka, E.; Grafenstein, J.; Gauss, J.; Reichel, F.; Olsson, L.; Konkoli, Z.; Cremer, D. *Program package COLOGNE 99*; Goteborg University: Goteborg, 1999.

(47) Guthrie, R. D.; Jenkins, I. D.; Yamasaki, R.; Skelton, B. W.; White, A. H. *J. Chem. Soc., Perkin Trans. 1* **1981**, 2328.

(48) Marton-Meresz, M.; Kuszmann, J.; Pelczer, I.; Parkanyi, L.; Koritsanszky, T.; Kalman A. *Tetrahedron* **1983**, *39*, 275.

(49) Trefonas, L. M.; Sato, T. *J. Heterocycl. Chem.* **1966**, *3*, 404.

(50) Dauban, P.; Chiaroni, A.; Riche, C.; Dodd, R. H. *J. Org. Chem.* **1996**, *61*, 2488.

(51) Bouř, P.; Sychrovský, V.; Maloň, P.; Hanzlikova, J.; Baumruk, V.; Pospišek, J; Buděšínský, M. *J. Phys. Chem. A* **2002**, *106*, 7321.

(52) Helgaker, T.; Jaszunski, M.; Ruud, K.; Górska, A. *Theor. Chem. Acc.* **1998**, *99*, 175.

(53) Bouř, P.; Buděšínský, M. *J. Chem. Phys.* **1999**, *110*, 2836.

(54) Gräfenstein, J.; Cremer, D. *Chem. Phys. Lett.* **2004**, *383*, 332.

(55) Haasnoot, C. A. G.; de Leeuw, F. A. A. M.; Altona, C. *Tetrahedron* **1980**, 36, 2783.